Supplementary Materials for

The Matricellular Protein TSP1 Promotes Human and Mouse Endothelial Cell Senescence through CD47 and Nox1

Daniel N. Meijles[1,2,†], Sanghamitra Sahoo[1,2], Imad Al Ghouleh[1,2,4], Jefferson H. Amaral[1,2], Raquel Bienes-Martinez[1], Heather E. Knupp[1], Shireen Attaran[2], John C. Sembrat[1,2], Seyed M. Nouraie[3] Mauricio M. Rojas[1,3], Enrico M. Novelli[1], Mark T. Gladwin[1,3], Jeffrey S. Isenberg[1,2,3], Eugenia Cifuentes-Pagano[1,2], and Patrick J. Pagano[1,2*]

*Corresponding author. Email: pagano@pitt.edu (PJP)

This PDF file includes:

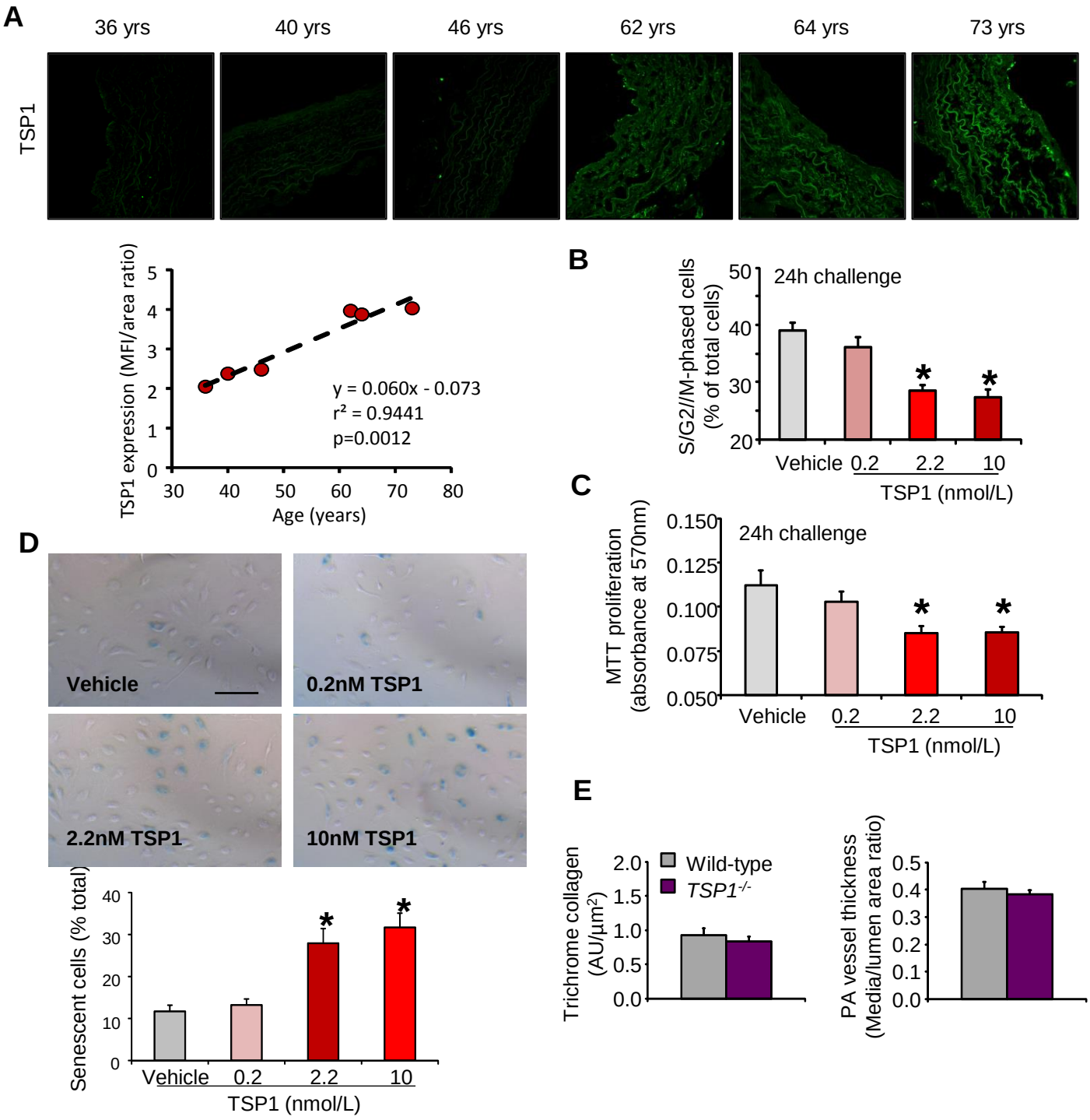

<u>Supplementary Figure S1:</u> TSP1 is increased in aging human lung vasculature and reduces endothelial cell proliferation. (**A**) Representative TSP1 abundance in control disease-free human pulmonary artery specimens detected by immunofluorescence (upper panels), measurements of fluorescence intensity (MFI) by ImageJ are plotted as linear regression, equation, r^2 and p values are indicated in the graph *(*lower panel). (**B** and **C**) TSP1 at concentrations of 2.2 and 10 nmol/L inhibit HPAEC cell cycle progression characterized by decreased percent of cells in S/G2/M phases by propidium iodide labeling and FACS (B), and proliferation measured using an ELISA plate-based MTT protocol (C). Data are mean ± SEM (n=4 [B] or 3 [C]), *p<0.05 compared to vehicle control by one-way ANOVA. (**D**) TSP1 at concentrations of 2.2 and 10 nmol/L promotes HPAEC senescence detected by SA-beta-Gal assay. Bar graph data are mean ± SEM (n=3), *p<0.05 compared to vehicle control by one-way ANOVA. (**E**) *TSP1*$^{-/-}$ does not alter pulmonary artery vessel collagen (left panel) or thickness (right panel) compared to wild-type controls at middle age. Data are mean ± SEM (n=3 animals/12 images per group).

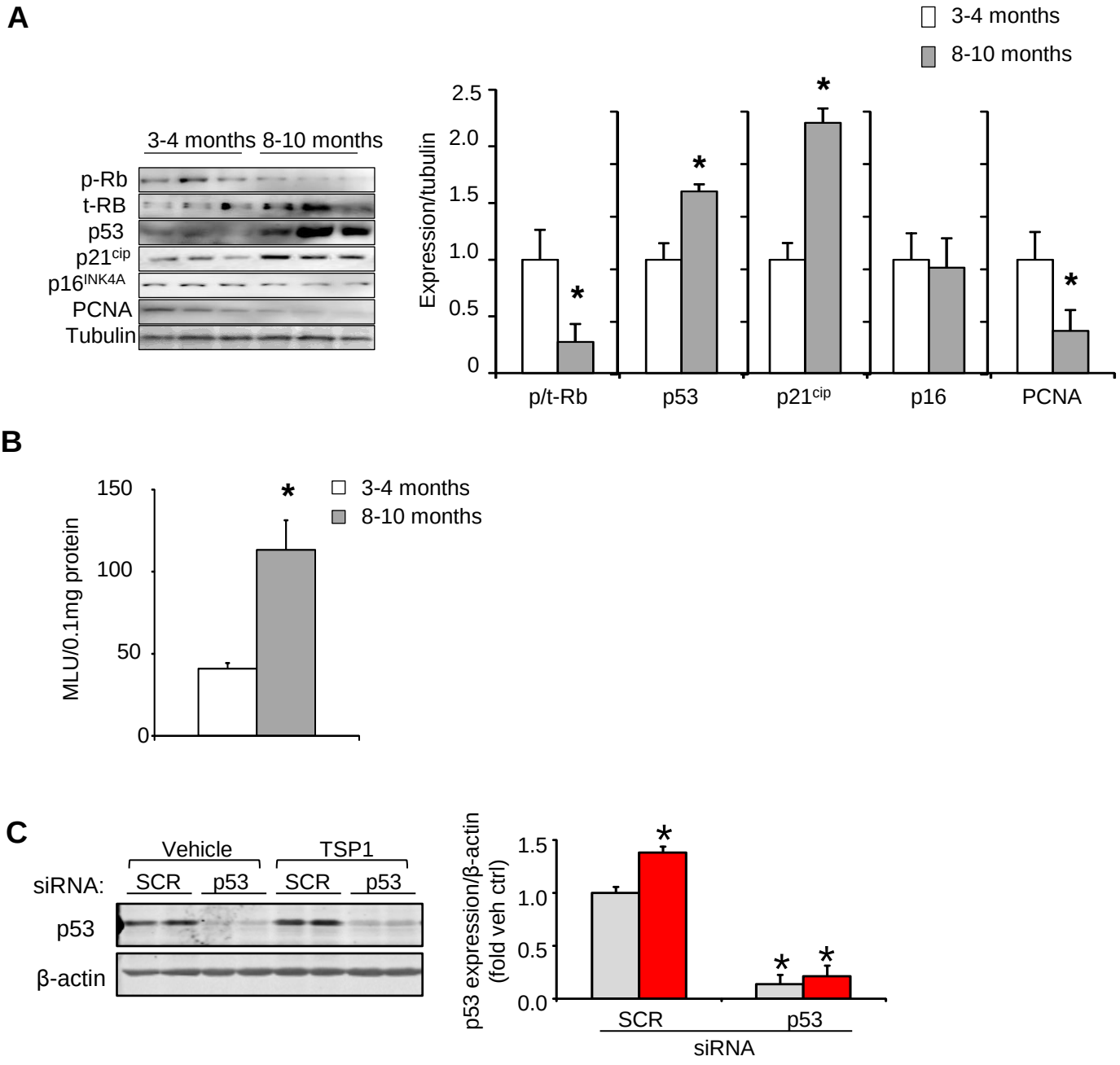

<u>Supplementary Figure S2:</u> Age-dependent changes in abundance of senescence markers in mice. (**A**) Confirmation that murine aging at middle age increases tissue senescence, consistent with increased p53 and p21^{cip} and decreased Rb phosphorylation and PCNA abundance, with p16INK4A amounts unaffected (Western blot). Graphs are mean ± SEM (n=6), *p<0.05 compared to vehicle control by Students *t*-test for each protein. (**B**) Murine aging increases superoxide production in wild-type animals assayed by lucigenin-enhanced chemiluminescence at middle age. Data are mean ± SEM (n=6); *p<0.05 compared to vehicle control by Students *t*-test. (**C**) p53 siRNA knockdown efficiency in HPAEC in the presence of vehicle or TSP1 (2.2 nmol/L; 24h). Left panels: representative Western blots for total-p53 and beta-actin. Right panel: quantitative analysis of p53 expression; data are mean ± SEM (n=3). *p<0.05 compared to scrambled siRNA (SCR) control by one-way ANOVA.

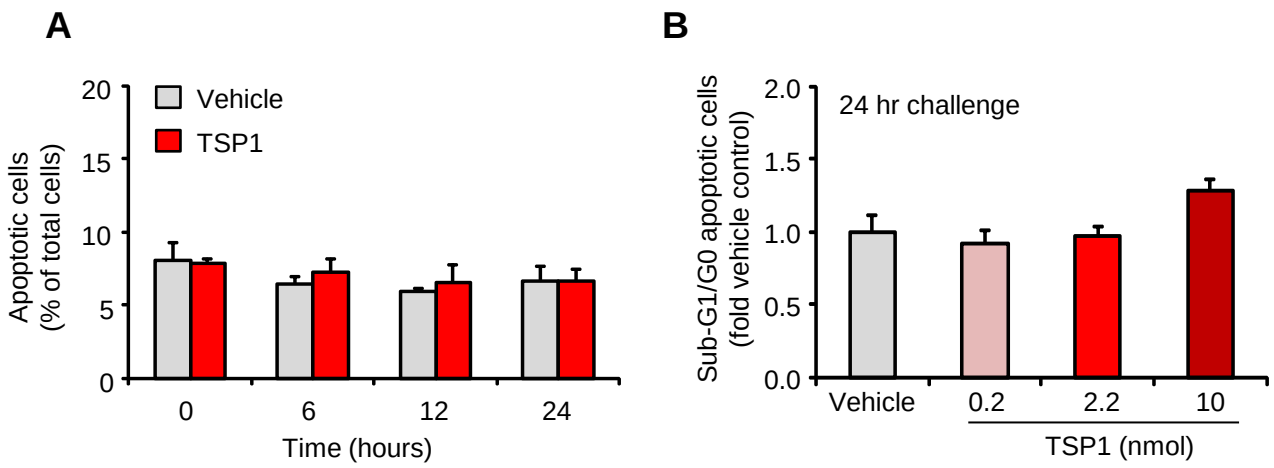

Supplementary Figure S3: TSP1 does not induce endothelial cell apoptosis. (**A** and **B**) TSP1 does not induce HPAEC apoptosis under the current experimental conditions at 2.2nmol/L measured kinetically using trypan-blue inclusion assay (A) or dose-dependently by FACS analysis (B). Data are mean ± SEM (n=3).

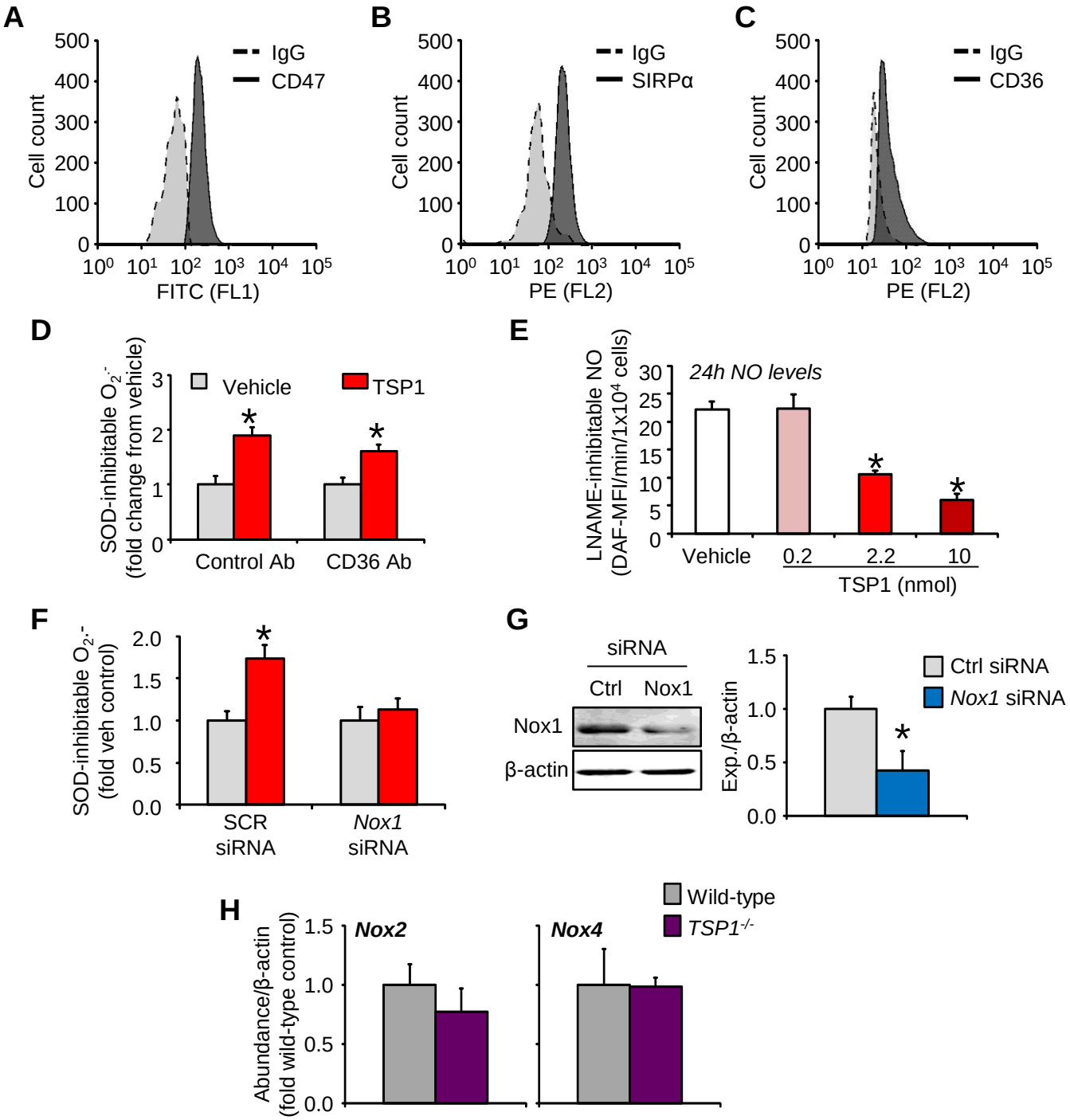

Supplementary Figure S4: The TSP1-CD47 axis selectively regulates Nox1. Comparative HPAEC abundance of (**A**) CD47, (**B**) SIRP-α and (**C**) CD36 measured by FACS. Histograms are representative of 3 experiments with 10,000 events recorded per detection. (**D**) CD36 blockade did not inhibit TSP1 induced $O_2^{\cdot-}$ production in HPAECs as measured by cytochrome c reduction. Data are mean ± SEM (n=3 biological replicates per treatment), *p<0.05 compared to vehicle treated controls by one-way ANOVA. (**E**) Effect of TSP1 (24hr) challenge on L-NAME-inhibitable NO production in HPAECs as measured by DAF fluorescence (MFI, mean intensity fluorescence) using a fluorescence plate reader. Data are mean ± SEM (n=3 biological replicates per treatment), *p<0.05 compared to vehicle treated controls by one-way ANOVA. (**F**) *Nox1* gene silencing siRNA inhibits TSP1-induced HPAEC $O_2^{\cdot-}$. Data are mean ± SEM (n=3 biological replicates per treatment), *p<0.05 for TSP1 challenge compared to vehicle control by one-way ANOVA. (**G**) Confirmation of Nox1 knockdown efficiency in HPAECs measured by Western blot. Data are mean ± SEM (n=3 biological replicates per treatment), *p<0.05 compared to control siRNA by Students *t*-test. (**H**) The abundance of Nox2 and Nox4 in middle-aged wild-type and TSP1$^{-/-}$ mice lungs measured by Western blot, normalized to β-actin. Data are mean ± SEM (n=6 mice per group).

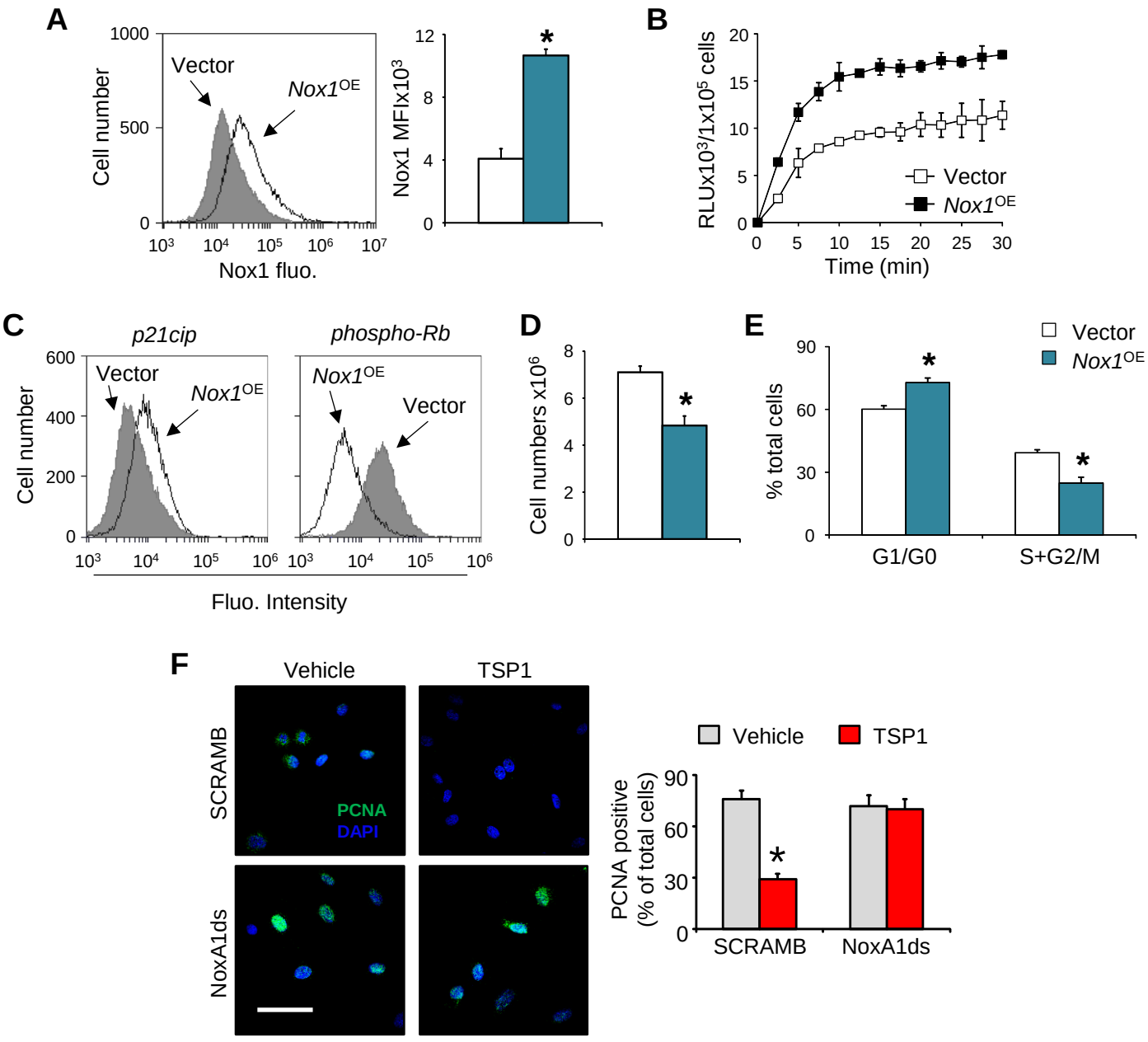

Supplementary Figure S5: Nox1 influences cell cycle progression and senescence. Human Nox1 overexpression (*Nox1*^{OE}) of HPAEC confirmed by FACS detection. Data are mean ± SEM (n=3), *p<0.05 compared to vector controls by Students *t*-test. (**B**) Nox1 overexpression increases $O_2^{\cdot-}$ generation in intact ECs detected by lucigenin-chemiluminescence. Data are mean ± SEM (n=3). (**C**) Nox1 overexpression increases p21^{cip} and decreases Rb phosphorylation detected by FACS labelling. Images are representative of 3 independent experiments. (**D**) Nox1 overexpression decreases EC proliferation assessed by trypan-blue exclusion assay. Data are mean ± SEM (n=3), *p<0.05 compared to vector controls - Students *t*-test. (**E**) Nox1 overexpression decreases cell cycle progression detected by propidium iodide-FACS labelling. Data are mean ± SEM (n=3), *p<0.05 compared to vector controls by Students *t*-test for each phase. (**F**) Treatment of HPAEC with NoxA1ds reverses TSP1-induced decrease in PCNA expression as assessed by immunofluorescence (PCNA, green; DAPI, blue). Data are mean ± SEM (n=3; 12-20 images per group; scale bar: 10µm); *p<0.05 for TSP1 challenge versus SCRAMB vehicle control by one-way ANOVA.

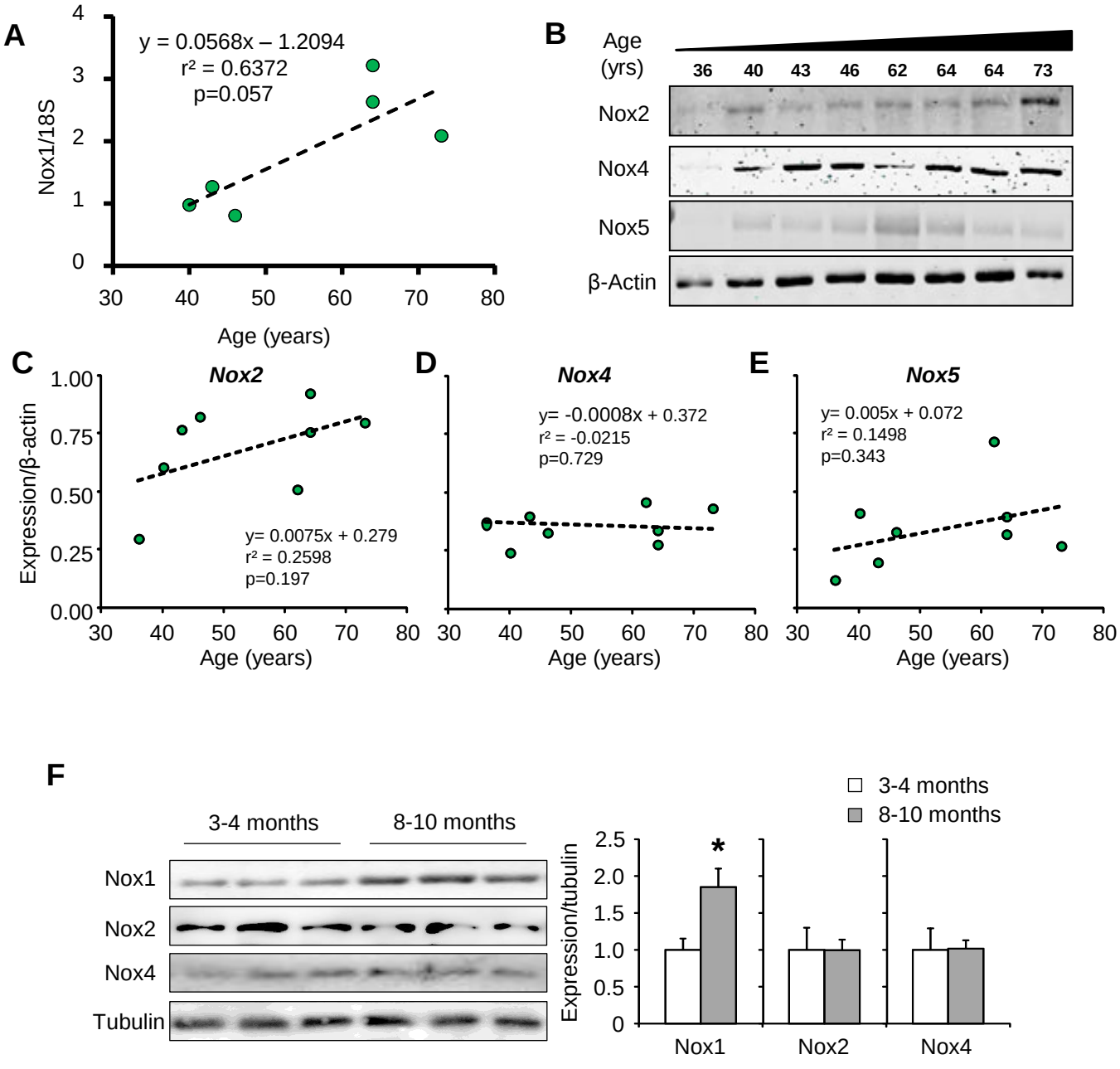

Supplementary Figure S6: Age-dependent changes in abundance of Nox isoforms in human and mouse lung samples. (**A**) Expression of *Nox1* mRNA significantly correlated with age in human lung homogenates as quantified by qRT-PCR. (**B** - **E**) Expression of Nox2, Nox4 and Nox5 protein in lungs of humans of various ages (B) normalized to beta-actin (C-E) as assessed by Western blot. Data are plotted as linear regression and equation, r^2 and p values are indicated in the corresponding graphs. (**F**) Expression of Nox1, Nox2 and Nox4 protein in aging murine lungs assessed by Western blot (left panels) normalized to alpha-tubulin (right panels). Data are mean ± SEM (n=6); *p<0.05 compared to vector controls by Students *t*-test for each protein.

Supplementary Table 1: Characteristics of pulmonary disease-free human samples.

Parameter	<50 yrs (n=4)	>50 yrs (n=4)
Mean age (SEM)	41.25 ± 2.13	65.75 ± 2.46
Range (years)	36 - 46 (10)	62 - 73 (11)
Male gender (%)	100	50
Smoking history	1/4	0/4
Av BMI (kg/m^2)	31.0 ± 1.6	32.3 ± 3.3

Supplementary Table 2: Cause of death and existence of non-pulmonary diseases of the human samples.

	Number (>50 yrs)
Stroke	4/8 (3/4)
Blunt trauma	4/8 (1/4)
Systemic hypertension*	4/8 (3/4)
Diabetes*	2/8 (1/4)